Mechanics of Advanced Composite Structures

Journal homepage: https://macs.semnan.ac.ir/

Semnan University

ISSN: 2423-7043

Research Article

Biodegradation, Mechanical and Physical Properties of Poly(butylene succinate) and Natural Rubber Compound Blend Filled with Activated Carbon from Coconut Fruit

Nuan La-ong Srakaew [a], Ing-orn Sittitanadol [b], Patcharapon Somdee [a], Sombut Noyming [a], Witawat Singsang [c], Pranee Chumsamrong [d], Natkrita Prasoetsopha [a]

[a] *Department of Materials and Medical Technology Engineering, Faculty of Engineering and Technology, Rajamangala University of Technology Isan, Nakhon Ratchasima, 30000, Thailand*

[b] *Department of Metallurgical Engineering, Faculty of Engineering, Rajamangala University of Technology Isan, Khon Kaen Campus, Khon Kaen, 40000, Thailand*

[c] *Department of Aircraft Part Manufacturing Technology, Faculty of Industrial Technology, Rambhai Barni Rajabhat University, Chanthaburi, 22000, Thailand*

[d] *School of Polymer Engineering, Institute of Engineering, Suranaree University of Technology, Nakhon Ratchasima, 30000, Thailand*

ARTICLE INFO

Article history:

Received: 2024-06-07
Revised: 2025-07-06
Accepted: 2024-05-12

Keywords:

Poly(butylene succinate);
Natural rubber;
Coconut;
Activated carbon.

ABSTRACT

Activated carbon (AC) was synthesized from coconut fruit and used as a bio-filler in poly(butylene succinate) (PBS) and natural rubber compound (NRC) composites. The activation process used a potassium hydroxide (KOH) solution, followed by microwave irradiation. Two KOH concentrations (1 M and 3 M) were used, and the obtained AC was labeled AC 1 M KOH and AC 3 M KOH. The objective of this study was to examine the effects of AC type and content (0-6 phr) on the mechanical, physical, and biodegradation properties of PBS/NRC/AC composites. The results showed that AC contained 73-74 % carbon content. The AC 3 M KOH exhibited a higher surface area. The mechanical properties of PBS/NRC/AC composites, including flexural strength, impact strength, tensile strength, Young's modulus, and elongation at fracture, tended to decrease with increasing amounts of AC. However, adding AC 3 M KOH had a more positive effect on these properties compared to AC 1 M KOH. The crystalline structure of PBS was not affected, while the melt flow index (MFI) of the composite tended to decrease with the addition of AC. The composite with 6 phr of AC 3 M KOH showed 22.4% CO_2 absorption, 35% degradation after 6 months, and 0.84% water absorption, all of which were higher than those observed for 6 phr of AC 1 M KOH. The surface morphology of PBS/NRC/AC composites had a rough appearance, with rubber particles and AC dispersed within the PBS matrix. The surface roughness intensified with increasing AC content.

1. Introduction

Currently, the demand for plastic products is rapidly expanding, leading to a significant rise in plastic waste after use, which has become a major environmental concern. Hence, considerable research efforts have focused on developing biodegradable plastics as a strategy for reducing plastic waste [1-5]. Biodegradable polymers are materials that can be decomposed under environmental conditions by microorganisms [3-6]. Examples of such polymers include poly(lactic

* **Corresponding author.**
E-mail address: natkrita.pr@rmuti.ac.th

Cite this article as:
Prasoetsopha, N. et al., 2025. Biodegradation, Mechanical and Physical Properties of Poly(butylene succinate) and Natural Rubber Compound Blend Filled with Activated Carbon from Coconut Fruit. *Mechanics of Advanced Composite Structures*, 12(1), pp. xx-xx
https://doi.org/10.22075/MACS.2024.39315.2050

acid) (PLA) [7-9], poly(caprolactone) (PCL) [9,10], and particularly poly(butylene succinate) (PBS) [2-5, 11], which is synthesized from monomers 1,4-butanediol and succinic acid. PBS is notable for its good mechanical properties and compatibility with conventional processing methods, although its high cost remains a major drawback. To reduce these costs, researchers have explored blending PBS with other materials [2, 11-14] or forming composites [3, 4, 15, 16]. Studies have shown that blending PBS with other materials can significantly improve its properties. For instance, P. Faibunchan et al. [12] reported that incorporating epoxidized natural rubber (ENR) into PBS enhanced its elongation. Similarly, N. Prasoetsopha et al. [17] reported that blending PBS with a natural rubber compound (NRC) at an 80/20 ratio resulted in the highest impact strength and elongation at break. Natural rubber, a renewable bio-based elastomer with high elasticity, has proven to be an ideal blend material for improving various properties of PBS and other polymers [2, 11-14].

Activated carbon (AC) is a porous carbonaceous material widely used in many applications, such as water treatment [18, 19], agriculture [20, 21], and energy storage [22-24]. It is often produced from biomass or waste materials, such as rice husks [23, 25], coconut shells [19, 22], corn [26], and coffee grounds [24], utilizing either physical or chemical activation methods [19, 22-26]. The chemical activation method is frequently preferred by researchers due to its low processing temperature, short processing time, and high efficiency [19, 23, 26]. The effectiveness of the chemical activation process depends on key factors, including the type and concentration of the activating agent. For example, E.H. Sujiono et al. [19] found that sodium hydroxide (NaOH) yielded the highest surface area for activated carbon derived from coconut shells compared to phosphoric acid (H_3PO_4) and zinc chloride ($ZnCl_2$). Additionally, M. Molina-Sabio and F. Rodriguez-Reinos [27] found that potassium hydroxide (KOH) enhanced microporosity, resulting in a more diverse micropore structure. Furthermore, increasing the concentration of the activating agent, such as potassium hydroxide (KOH), has been shown to significantly enhance the surface area of activated carbon, as demonstrated in the activation of rice husk [23].

While the production of activated carbon from agricultural waste, such as coconut shells, has been extensively studied, other by-products of coconut, particularly coconut fruits, remain underutilized. Current literature predominantly focuses on well-known biomass sources, overlooking the potential of lesser-studied agricultural residues. Using these biodegradable by-products to develop composite materials not only improves the properties of the composites but also contributes to sustainable waste management by adding value to agricultural waste and mitigating environmental pollution associated with conventional waste disposal methods.

In this research, the effects of potassium hydroxide concentration on the characteristics of activated carbon derived from coconut waste were studied. Additionally, the study examined how different amounts of activated carbon influenced the mechanical and physical properties of PBS/NRC/AC composites. The biodegradability of the resulting composites was also evaluated.

2. Materials and Methods

Coconut fruit waste was obtained from a farm in Ratchaburi Province, Thailand. Figure 1 shows the raw material of coconut waste obtained from the coconut fruit, which consists of both the coconut husk and shell. Poly(butylene succinate) (PBS) (BioPBS™ FZ71PM grade) was procured from PTT MCC Biochem Company Limited. The melt flow rate of PBS was 24.2 g/10 minutes. Potassium hydroxide (KOH, Kemaus, 85%) was used in the activation process, while hydrochloric acid (HCl, Labo Chemie PVT. LTD., 35.4%) was used for neutralization. Commercial-grade natural rubber (STR 5L) and chemical reagents, including stearic acid, zinc oxide (ZnO), tetramethylthiuram disulfide (TMTD), and sulfur (S), were used. Rubber and all chemical reagents were supplied by Chareon Tut Co., Ltd.

Fig. 1. Coconut waste obtained from coconut fruit (consisting of coconut husk and coconut shell)

2.1. Activated Carbon Preparation

The coconut fruit was pyrolyzed in a conventional pyrolysis furnace at 600°C for 4 to 6 hrs. After cooling, the obtained biochar was milled and passed through a 270-mesh sieve. The particle size of the biochar, determined using a particle size analyzer (FRITSCH, PARTICLE SIZER ANALYSETTE 22 NanoTec), was found to be 23.3 ± 1.7 μm. The biochar was activated using a potassium hydroxide (KOH) solution and microwave irradiation, enhancing activation through chemical and rapid thermal treatment. Two KOH concentrations, 1 M and 3 M, were used to compare the effect of KOH concentration on

the properties of AC, as high KOH concentration can improve the surface area of AC [28]. Figure 2 illustrates the activation process. In this process, the biochar was soaked in a KOH solution for 24 hrs and then heated in a microwave oven at 600 watts for 6 minutes. Previous research by H. Dang et al. [29] showed that using high microwave power (480-660 watts) creates activated carbon (AC) with more pore space and surface area compared to low power, and K.Y. Foo and B.H. Hameed [30] found that the surface area of AC grows when the microwave heating time is increased to 6 minutes. After that, it was neutralized using HCl and washed with deionized water to remove excess salt. Finally, the AC was dried in a hot air oven at 60˚C for 24 hrs.

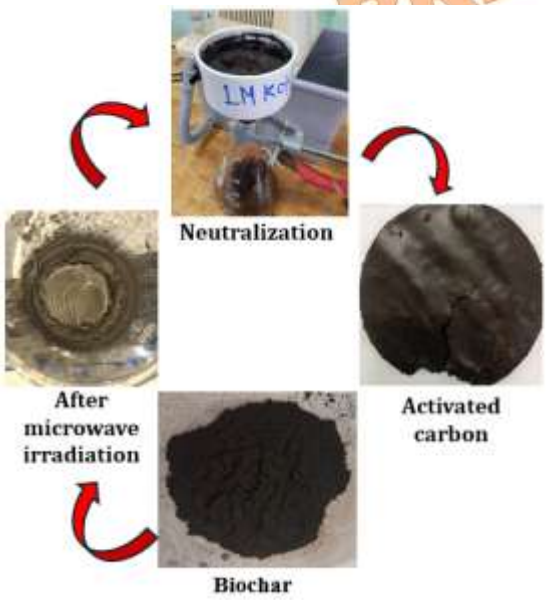

Fig. 2. Activation process

2.2. Activated Carbon Characterization

The morphology and chemical composition of the AC were investigated using a scanning electron microscope (SEM, AURIGA, Carl Zeiss) coupled with energy-dispersive spectroscopy. The particle size of AC was determined using a laser scattering particle size analyzer (HORIBA, LA–950V2). The specific surface area and total pore volume of the AC were determined using nitrogen adsorption Brunauer–Emmett–Teller (BET), with the samples degassed at 300˚C for 6 hrs.

2.3. Preparation of Natural Rubber Compound

Table 1 shows the order of rubber and chemical reagents used in the preparation of a natural rubber compound (NRC) on a two-roll mill. The natural rubber and chemical reagents were used as received. In the compounding process, natural rubber was masticated for 10 minutes, followed by the sequential addition of the chemical reagents every 4 minutes. After being thoroughly mixed, the NRC was kept at room temperature for 24 hrs before use.

Table 1. Natural rubber compound formula

Order	Chemical reagent	Amount (phr)
1	NR	100
2	Stearic Acid	2.5
3	ZnO	5
4	TMTD	0.7
5	S	2.5

2.4. Sample Preparation

PBS and NRC were mixed in a constant ratio of 80/20 by weight, with varying amounts of AC added at concentrations of 0, 2, 4, and 6 phr. To prepare for the mixing process, PBS was dried in a convection oven at 50˚C for 24 hrs to reduce the moisture content. In the mixing process, PBS, NRC, and AC were melted and combined using an internal mixer (MX500–D75L90, Chareon Tut Co., Ltd., Thailand) at 145˚C for 15 minutes with a rotor speed of 50 rpm. The total weight of each batch was 270 grams. After the composites cooled, they were ground with a plastic grinder.

In the compression process, the ground samples were pressed using a hot compression molding machine (PR2D-W300L350 PM-WCL-HMI, Chareon Tut Co., Ltd., Thailand) at 145˚C with 1500 psi pressure. A stainless-steel mold was used during this process. The compression process involved three steps: preheating, pressing, and cooling for 5, 3, and 3 **minutes**, respectively. The preparation process of PBS/NRC/AC composites is shown in Fig. 3.

2.5. Mechanical Testing

The tensile testing was conducted using a dumbbell-shaped specimen prepared according to ASTM D638-10. A universal testing machine (LS Plus Series, Lloyd) with a load cell of 10 kN was used to perform the tests. A crosshead speed of 50 mm/min was used, and the tests were conducted at room temperature. Five specimens were conducted for each ratio.

The three-point bending tests were conducted using the universal testing machine (LS Plus Series, Lloyd) with a load cell of 10 kN, following ASTM D790-03. The test was conducted at a crosshead motion rate of 1.28 mm/min and a support span of 48 mm, all at room temperature. For each composition ratio, five specimens were tested to obtain an average value.

The notched Izod impact test was performed using an impact tester at room temperature following ASTM D256-04 (Ceast 9050, INSTRON). Five specimens were evaluated.

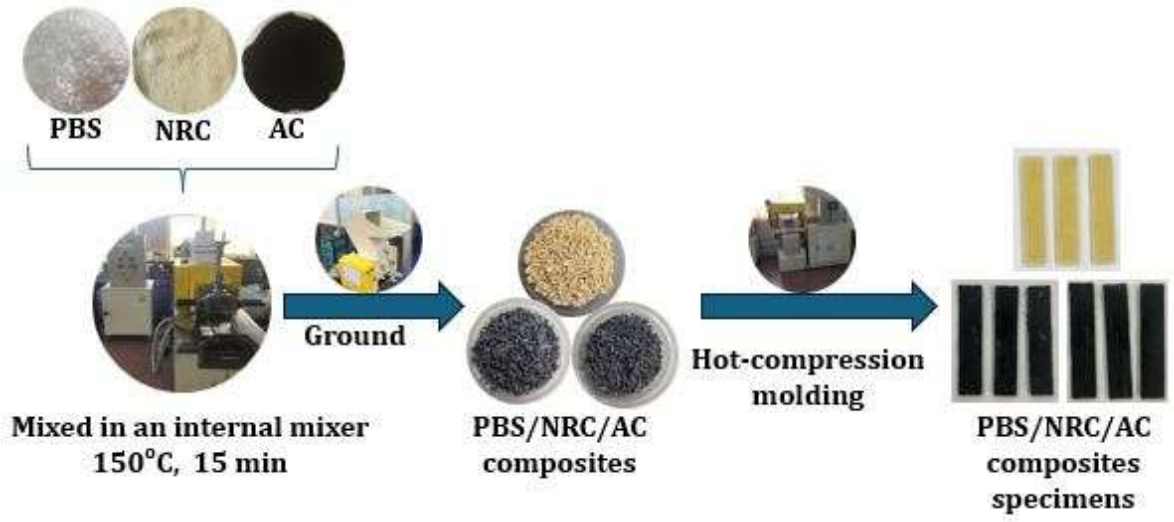

Fig. 3. Illustration of the preparation process for PBS/NRC/AC composites

2.6. Morphology

The fractured surface of the tested impact specimens was examined using a scanning electron microscope (SEM, AURIGA, Carl Zeiss). The sample was coated with gold to improve its conductivity and reduce the charging effects. An electron accelerating voltage of 10 kV and a vacuum pressure of 4.4×10^{-4} mbar were applied.

2.7. Physical Testing

The crystalline regions of PBS were investigated using X-ray diffraction (XRD, D8 Advance, Bruker, Germany). The diffraction patterns were obtained over a 2 theta (2θ) range of 5-80 degrees with a scan step of 0.02°/s.

The melt flow index (MFI) of the composites was measured by using a melt flow indexer (mi2.1, GÖTTFERT, Germany). Prior to measurement, the samples were dried in a hot air oven at 50°C for 24 hrs. The sample was extruded through a die according to ASTM D1238-10, with a load of 2.16 kg applied at 150°C.

The water absorption measurement was conducted according to ASTM D570 using a sample with the dimensions of 20 mm, 10 mm, and 3 mm. Prior to being used, the sample was dried at 50°C overnight. The dried sample was then weighed and soaked in deionized water for 24 hrs. The sample was subsequently taken out of the water and tapped on a paper towel to remove excess surface water. The sample was then reweighed. The percentage of water absorption (W.A.) was calculated according to Eq. (1) [31], where W_i and W_f are the initial and final masses, respectively.

$$W.A.(\%) = \frac{W_f - W_i}{W_i} \times 100 \quad (1)$$

For the odor absorption test, a sample size of 20 mm × 100 mm × 0.3 mm was used. The CO_2 absorption measurement was carried out in a simulated box, where the CO_2 level was measured using a CO_2 digital monitor. In the process, incense sticks were used to generate the CO_2 in the simulated box, and the CO_2 concentration was allowed to stabilize. The sample was then introduced, and the initial CO_2 value was recorded. After 70 minutes, the final CO_2 value was recorded. This method is based on the approach described by P. Somdee et al. [32]. The percentage of CO_2 absorption (Abs) was calculated using Eq. (2) [33], where A_i and A_f are the initial and final CO_2 values, respectively.

$$\text{Abs}(\%) = \frac{A_i - A_f}{A_i} \times 100 \quad (2)$$

2.8. Biodegradation Test

For the biodegradation test, a sample size of 20 mm x 10 mm x 3 mm was used. The samples were dried in an oven at 60°C for 24 hrs and weighed as w_o. Then, the samples were buried in potting soil at a depth of 5 cm, as shown in Fig. 4. The soil had a pH range of 6-7.6 and a moisture content of 50-70% of the dry soil weight, which was regularly monitored using a calibrated moisture meter. Water was added as needed to maintain the moisture. Five specimens were used for each ratio. The samples were examined at 2, 4, and 6-month intervals. When taking samples out, the surrounding soil was carefully dug out to avoid damage to the samples. The samples were then gently washed with distilled water to remove any soil residue and dried in an oven at 60°C until a constant weight was achieved (approximately 24 hrs). The sample was then weighed as w_f. An analytical balance with a precision of 0.001 mg was used for weighing. This

method is based on the approach described by R. Siakeng et al. [34]. The percentage weight loss (W_{loss}) was calculated using Eq. (3) [35].

$$W_{loss}(\%) = \frac{w_o - w_f}{w_o} \times 100 \quad (3)$$

Fig. 4. Biodegradation test

3. Results and Discussion

3.1. Activated Carbon Characteristics

Figure 5 shows the morphology of activated carbon. It could be seen that both ACs exhibited a flake-like shape with varying particle sizes. The chemical composition of the AC is shown in Table 2. The major and minor elements of the AC were carbon (C) and oxygen (O). These results are consistent with the previous report, where C and O content ranged between ~65-75% and ~20-25%, respectively [36]. Other elements present included potassium (K) and magnesium (Mg).

The particle size distribution of ACs obtained using the laser scattering technique is shown in Fig. 6. The analysis results revealed that the average particle sizes of AC 1 M KOH and AC 3 M KOH were 16.28 ± 1.66 μm and 18.09 ± 1.76 μm, respectively. The particle size of AC 1 M KOH was slightly smaller than that of the AC 3 M KOH, although both ACs exhibited similar shapes. However, they both have smaller particle sizes compared to the raw materials (23.3 ± 1.7 μm).

The nitrogen adsorption Brunauer–Emmett–Teller (BET) results are presented in Table 3. The surface areas (S_{BET}) of AC 1 M KOH and AC 3 M KOH were 11.80 and 18.27 m^2/g, respectively. Additionally, the total pore volumes of AC 1 M KOH and AC 3 M KOH were 0.0094 cm^3/g and 0.0128 cm^3/g, respectively. It is evident that the surface area and total pore volume of AC 3 M KOH were higher than those of AC 1 M KOH. This difference can be attributed to the higher concentration of KOH, which induced the formation of micropores, resulting in an increased surface area and total pore volume [37]. A higher surface area tends to enhance the mechanical properties by providing more surface area for interaction between the filler and the rubber matrix [38]. This result was expected, which corresponded with a previous report [23].

3.2. Mechanical Properties

The flexural strength of the composites, shown in Fig. 7, revealed that the addition of AC decreased the flexural strength. This reduction might be due to the increased amounts of AC, which led to the formation of large surface irregularities (microcracks). These irregularities cause increased stress, resulting in decreased mechanical properties [39]. This finding is consistent with the study by C. Veranitisagul et al. [40], which reported that increasing the content of nanosilver-coated carbon black (AgCB) in PBS led to a decrease in flexural strength. Additionally, the addition of AC 3 M KOH showed higher flexural strength compared to those prepared with AC 1 M KOH.

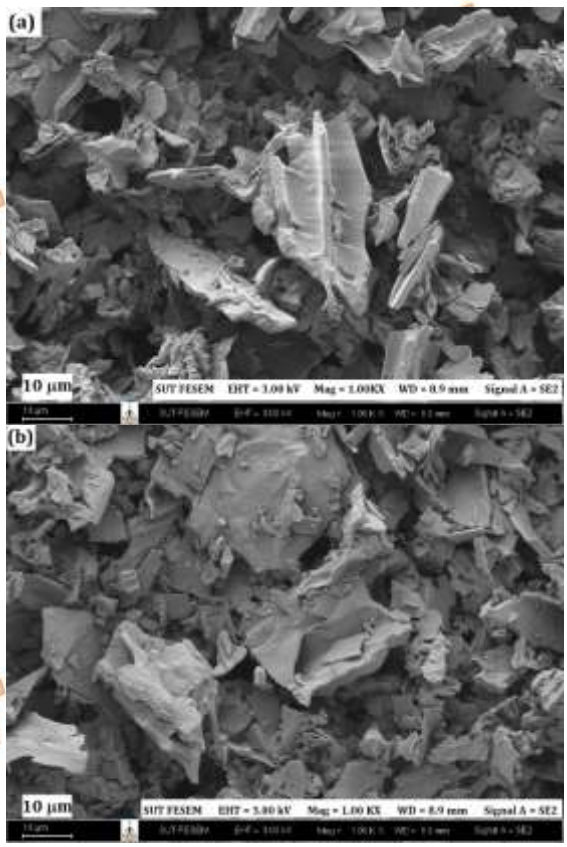

Fig. 5. SEM micrograph of activated carbon; (a) AC 1M KOH, (b) AC 3 M KOH

Figure 8 shows the impact strength of PBS/NRC/AC composites. It was observed that increasing the activated carbon content reduced the impact strength, which can be due to the improper interfacial adhesion between the AC and PBS matrix. This poor adhesion leads to the formation of microcracks, facilitating crack propagation during impact [41]. Composites with

lower AC 3 M KOH content exhibited higher impact strength compared to those with AC 1 M KOH. Conversely, at higher AC contents, AC 1 M KOH demonstrated better impact strength compared to AC 3 M KOH. Notably, at 2 phr of AC 3 M KOH, the impact strength reached 24 kJ/m^2, which is significantly higher than the 4.8 kJ/m^2 observed in PBS composites with 2 wt% waste coffee ground-derived activated carbon, as reported in the study by W. Singsang et al. [24].

Table 2. The elemental composition of coconut fruit biochar and activated carbon

Element content (%)	Coconut biochar	AC 1 M KOH	AC 3 M KOH
C	75.70	74.03	73.03
O	20.14	24.18	24.39
K	1.24	1.48	2.34
Mg	0.29	0.32	0.25
Na	0.63	-	-
F	1.26	-	-
Cl	0.75	-	-

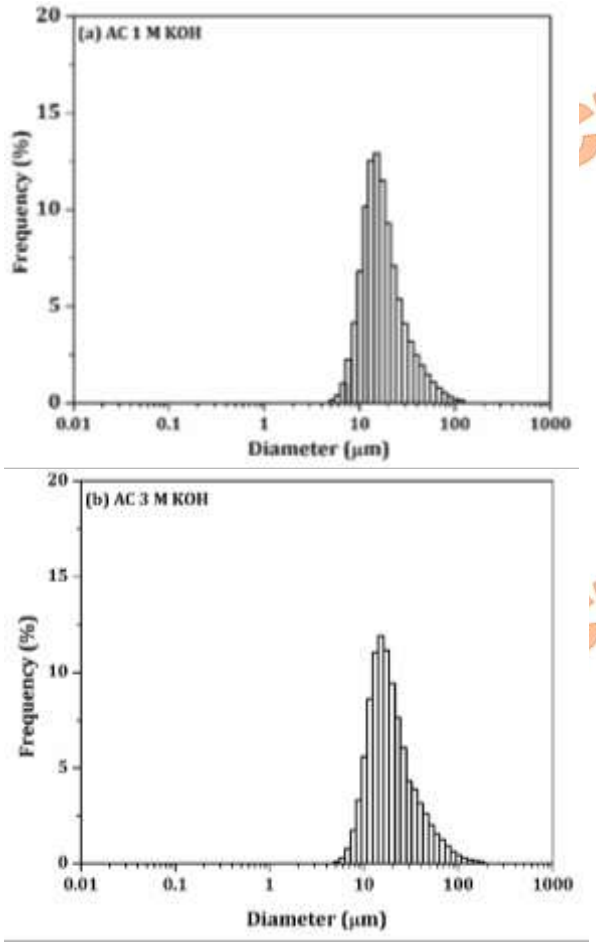

Fig. 6. Particle size distribution of activated carbon; (a) AC 1M KOH (b) AC 3 M KOH

Table 3. Surface area (S_{BET}) and total pore volume

Filler	S_{BET} (m^2/g)	Total pore volume (cm^3/g)
AC 1 M KOH	11.80	0.0094
AC 3 M KOH	18.27	0.0128

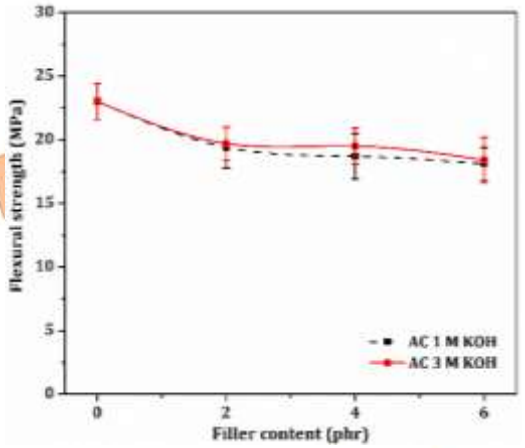

Fig. 7. Flexural strength of PBS/NRC/AC composites.

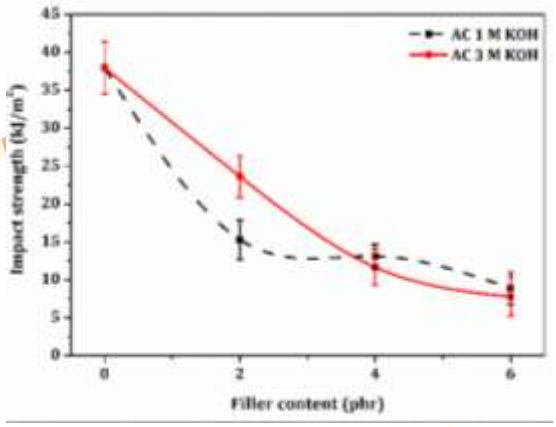

Fig. 8. Notched Izod impact strength of PBS/NRC/AC composites.

The tensile properties of PBS/NRC/AC composites, shown in Fig. 9, demonstrated that tensile strength tended to decrease with an increase in the content of activated carbon (see Fig. 9(a)). This result showed the same trend as inorganic filler in the PBS matrix [41, 42]. However, the addition of AC 3 M KOH showed a higher tensile strength compared to that of AC 1 M KOH. Notably, the addition of AC 3 M KOH resulted in a more significant increase in Young's modulus compared to the addition of AC 1 M KOH (Fig. 9(b)). Moreover, the elongation at break of PBS/NRC/AC composites followed the same trend as the tensile strength and Young's modulus (Fig. 9(c)). These composites exhibited lower mechanical properties than polybutylene succinate composites with 1 wt% biochar, as reported by S. Noh et al. [43], and lower than poly(butylene succinate-co-adipate) composites with 5 wt% biochar derived from wood residue,

as reported by M. Cappello et al. [44]. These lower mechanical properties can be attributed to the incompatibility between the AC and the PBS matrix [45].

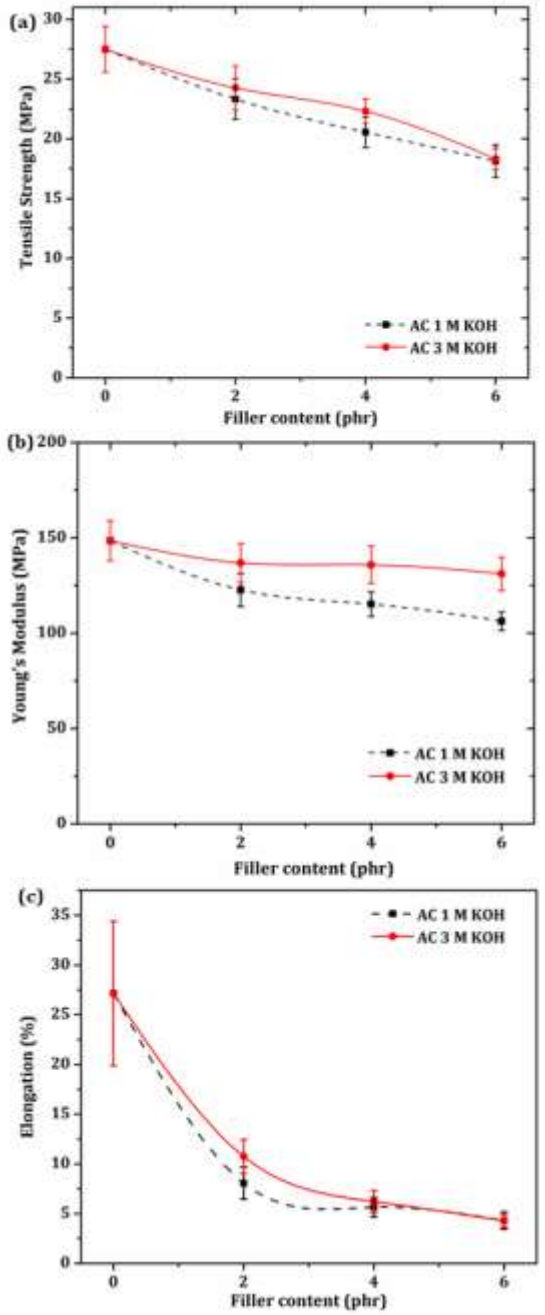

Fig. 9. Tensile properties of PBS/NRC/AC composites; (a) tensile strength; (b) Young's modulus; (c) elongation

3.3. Morphology

Figure 10 illustrates the morphology of PBS/NRC/AC composites. The PBS/NRC/AC composites exhibited a well-dispersed phase of NRC within the polymer matrix, as indicated by the red arrows in Fig. 10(a)-(g). The NRC particles were less than 10 µm, consistent with previous findings [17]. The activated carbon particles were also well dispersed in the matrix; however, incompatibility between the activated carbon and the PBS matrix, indicated by blue arrows in Fig. 10(a)-(f), led to a reduction in mechanical properties as the AC content increased. No significant morphological differences were observed when activated carbon prepared with different potassium hydroxide concentrations was used. Additionally, higher AC content roughened the surface, causing stress concentrations, further contributing to the decline in mechanical properties.

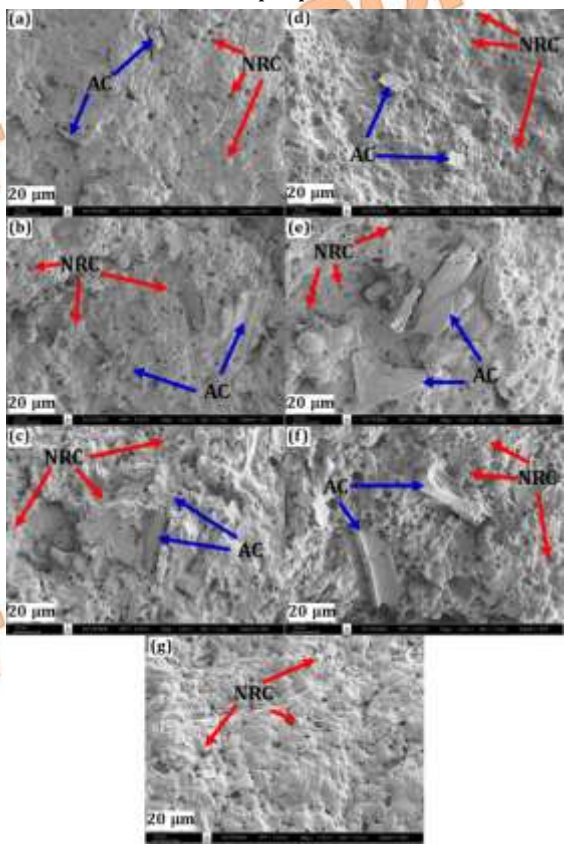

Fig. 10. SEM morphology of PBS/NRC/AC composites with varying amounts of AC; AC 1M KOH of: (a) 2 phr; (b) 4 phr; (c) 6 phr; AC 3 M KOH of: (d) 2 phr; (e) 4 phr; (f) 6 phr; and (g) 0 phr

3.4. Physical Properties

The XRD diffraction patterns of PBS/NRC/AC composites are shown in Fig. 11. All composites showed the diffraction peak at 19°, 22°, and 28°, which correspond to the (020), (110), and (111) crystallographic planes of PBS, respectively. These findings align with the previous studies by F. Ge et al. [46] and C. Veranitisagul et al. [40], which reported similar diffraction peaks for neat PBS and PBS composites. The consistent peak positions indicate that the addition of activated carbon did not alter the crystalline structure of the PBS matrix, suggesting that the filler had minimal influence on the matrix's crystallinity.

Table 4 illustrates the melt flow index (MFI) of PBS/NRC/AC composites. The results indicate that the MFI of the neat PBS/NRC composite was 2.79 g/10 mins. The addition of activated carbon derived from coconut fruit decreased the MFI, indicating that the presence of activated carbon

increases the viscosity. Increasing the activated carbon content further raises the viscosity, thereby lowering the MFI due to the accumulation formed within the matrix [47]. This finding is consistent with previous studies, such as those by C. Veranitisagul et al. [40], who reported that the inclusion of nanosilver-coated carbon black in PBS increased melt viscosity, leading to a decreased MFI. Similarly, K. Papadopulou et al. [48] found that increasing the biochar content from miscanthus straw to PBS composites resulted in higher viscosity and lower MFI due to enhanced interactions between the polymer matrix and the filler. Additionally, it can be observed that the MFI decreased more with the addition of AC 1 M KOH compared to AC 3 M KOH. This is likely because AC 1 M KOH has a slightly smaller particle size than AC 3 M KOH, as shown in the particle size test results. Smaller particles tend to accumulate more than larger particles [49].

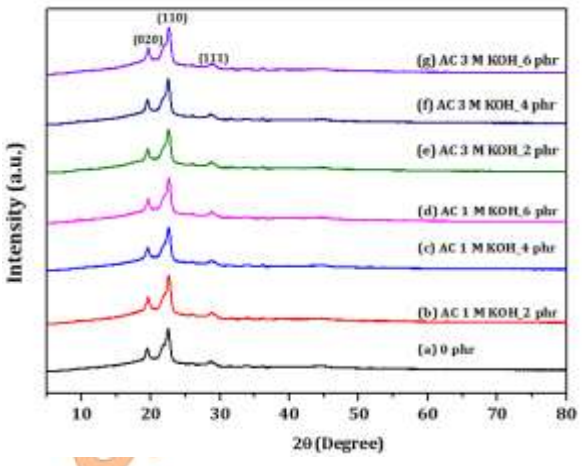

Fig. 11. XRD diffraction patterns of PBS/NRC/AC composites.

Table 4. Melt flow index

AC content (phr)	Melt flow index (g/10 mins)	
	AC 1 M KOH	AC 3 M KOH
0	2.79 ± 0.51	2.79 ± 0.51
2	2.77 ± 0.50	2.86 ± 0.52
4	2.55 ± 0.47	3.43 ± 0.64
6	1.71 ± 0.32	2.38 ± 0.44

The result of the odor absorption of PBS/NRC/AC composites is shown in Fig. 12. A blank test, which did not include the sample, was used as a control. The results show that the PBS/NRC/AC composites tended to increase the percentage of CO_2 absorption when the activated carbon was added. Specifically, the percentage of CO_2 absorption for the sample with AC 1 M KOH and AC 3 M KOH at 6 phr was 23.8% and 22.4%, respectively, representing an enhancement of two times compared to neat PBS/NRC composites. Moreover, PBS/NRC/AC composites showed a higher percentage of CO_2 absorption compared to composites made from natural rubber and spent coffee grounds [32], due to the higher porosity and surface area of the activated carbon. These composites could be used in packaging materials to extend the shelf life of perishable goods by absorbing CO_2 and other odor-causing gases, which are common in food storage environments.

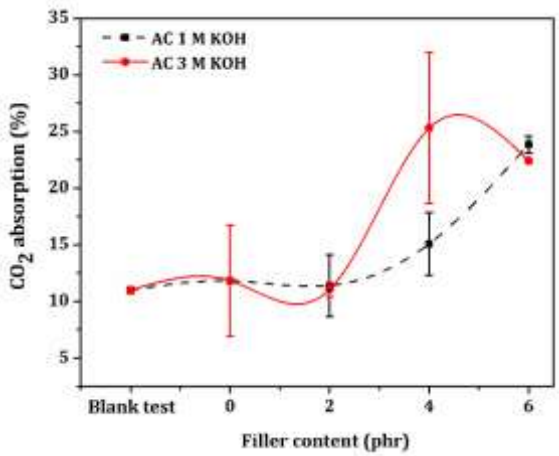

Fig. 12. CO_2 absorption of PBS/NRC/AC composites.

Table 5. Water absorption of PBS/NRC/AC composites.

AC content (phr)	Water absorption (%)	
	AC 1 M KOH	AC 3 M KOH
0	0.55 ± 0.05	0.55 ± 0.05
2	0.63 ± 0.02	0.62 ± 0.01
4	0.66 ± 0.03	0.74 ± 0.01
6	0.74 ± 0.01	0.84 ± 0.01

Table 5 shows the water absorption results. It can be seen that the addition of activated carbon increased water absorption. An increase in AC content led to a higher percentage of water absorption because activated carbon is highly porous, and higher AC content provides numerous micropores available for water absorption. This aligns with the findings of A. S. Mohammed Ali et al. [50], who reported that high carbon content can lead to significant water absorption, consistent with previous work showing that increased filler content in polymer composites is associated with higher water absorption [51]. The water absorption of the AC 3 M KOH samples was slightly higher than that of the AC 1 M KOH samples, which may be due to the AC 3 M KOH having a higher surface area and total pore volume available for water absorption compared to AC 1 M KOH [52].

3.5 Biodegradation Property

Figure 13 illustrates the degradation result of PBS/NRC/AC composites over 2, 4, and 6 months. The weight loss of PBS/NRC/AC composites tended to increase with an increase in the AC content. The porous nature of the activated carbon facilitates microbial activity and the fragmentation of the composites [53]. For the 2-month period, the percentage of weight loss of AC 3 M KOH was slightly higher than that of AC 1 M KOH. The difference may be due to the higher surface area, which provides more contact points for microbes to attach to samples and initiate the degradation process [54]. At 4 and 6 months, the percentages of weight loss for AC 1 M KOH and AC 3 M KOH were not significantly different. Additionally, longer degradation test periods showed a higher percentage of weight loss, which is consistent with a previous report [3]. This result aligns with the study by C. Veranitisagul et al. [40], which found that increasing the content of nanosilver-coated carbon black (AgCB) in PBS resulted in a higher percentage of weight loss in composites. These findings indicate that the PBS/NRC blends filled with activated carbon have good mechanical properties and are naturally degradable, making them suitable for applications such as soil cover films or biodegradable nursery bags.

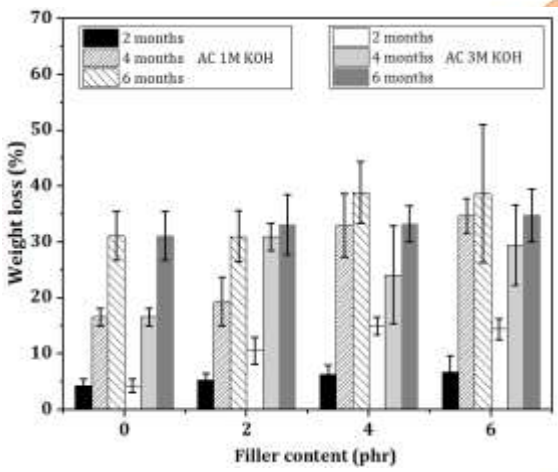

Fig. 13. Biodegradation of PBS/NRC/AC composites

4. Conclusions

Activated carbon derived from coconut fruit waste was successfully prepared using potassium hydroxide (KOH) solution and microwave irradiation and was then used as a bio-filler in poly(butylene succinate) (PBS) and natural rubber compound (NRC) blends.

The study revealed that KOH concentration significantly affects the properties of activated carbon:

- Lower concentrations resulted in smaller particles.
- Higher concentrations led to a larger surface area and total pore volume.

In PBS/NRC/AC composites:

- Increasing the AC content adversely impacted mechanical properties, likely due to poor filler-matrix compatibility.
- The crystalline structure of the polymer matrix remained largely unchanged.
- Using AC prepared with a higher KOH concentration improved mechanical properties, including flexural strength, impact strength, tensile strength, Young's modulus, and elongation, while also enhancing CO_2 absorption, water absorption, and biodegradability of the composites.

The findings suggest that PBS/NRC/AC composites are viable biodegradable materials, highlighting their potential for sustainable material development and application, such as soil cover films or biodegradable nursery bags. The type of coconut waste utilized may affect the characteristics of these blends, indicating possibilities for further study in developing biodegradable composites from alternative waste materials combined with rubber to enhance their properties and sustainability.

Nomenclature

PBS	Poly(butylene succinate)
PLA	Poly(lactic acid)
PCL	Poly(caprolactone)
PHB	Poly(hydroxybutyrate)
NRC	Natural rubber compound
AC	activated carbon
M	Molar
g	Gram
phr	Parts per hundred resin
w/w	Percentage weight per weight
m^2	Square millimetre
cm^3	Cubic centimetre
μm	Micrometre
MPa	Mega Pascal
°	Degree

s	Second
min	minute
hr	hour
˚C	Degree celsius
KOH	Potassium hydroxide
STR	Standard Thai Rubber
ZnO	Zinc Oxide
TMTD	Tetramethylthiuram disulfide
XRD	X-ray diffraction
HCl	Hydrochloric acid
CO_2	Carbon dioxide
C	Carbon
O	Oxygen
K	Potassium
Mg	Magnesium
BET	Brunauer–Emmett–Teller
MFI	Melt flow index
S_{BET}	Surface area

Acknowledgments

The author would like to thank all staff from the Faculty of Engineering and Technology, Rajamangala University of Technology Isan, Nakhon Ratchasima.

Funding Statement

This research project is supported by Thailand Science Research and Innovation (TRSI). Contract No. FF66-P1-109.

Conflicts of Interest

The authors declare no competing interests.

References

[1] Tokiwa, Y., Calabia, B., Ugwu, C. and Aiba, S., 2009. Biodegradability of Plastics. *International Journal of Molecular Sciences, 10*, pp. 3722–3742. Doi:10.3390/ijms 10093722

[2] Faibunchan, P., Pichaiyut, S., Kummerlowe, C. Vennemann, N. and Nakason, C., 2020. Green biodegradable thermoplastic natural rubber based on epoxidized natural rubber and poly(butylene succinate) blends: Influence of blend proportions. *Journal of Polymers and the Environment, 28*(3), pp. 1050-1067. Doi:10.1007/s10924-020-01655-5

[3] Sasimowski, E., Majewski, L. and Grochowicz, M., 2023. Study on the biodegradation of poly(butylene succinate)/wheat bran biocomposites. *Materials, 16*(21), p. 6843. Doi:10.3390/ ma16216843

[4] Huang, Z., Qian, L., Yin, Q., Yu, N., Liu, T. and Tian, D., 2018. Biodegradability studies of poly(butylene succinate) composites filled with sugarcane rind fiber. *Polymer Testing*, *66*, pp. 319–326. Doi:10.1016/ j.polymertesting.2018.02.003

[5] Zhao, J., Wang, X., Zeng, J., Yang, G., Shi F. and Yan, Q., 2005. Biodegradation of Poly(Butylene Succinate) in Compost. *Journal of Applied Polymer Science, 97*(6), pp. 2273–2278. Doi:10.1002/app.22009

[6] Samir, A., Ashour, F. H., Hakim, A. A. A. and Bassyouni, M., 2022. Recent advances in biodegradable polymers for sustainable applications. *npj Materials Degradation, 6*(1), p. 68. Doi:10.1038/s41529-022-00277-7

[7] Rong-or, C., Pongputthipat, W., Ruksakulpiwat, Y. and Chumsamrong, P., 2024. Soil burial degradation of bio-composite films from poly(lactic acid), natural rubber, and rice straw. *Polymer bulletin.* Doi:10.1007/s00289-024-05229-6

[8] Pongputthipat, W., Ruksakulpiwat, Y. and Chumsamrong, P., 2023. Development of biodegradable biocomposite films from poly(lactic acid), natural rubber and rice straw. *Polymer bulletin*, *80*(9), pp. 10289-10307. Doi:10.1007/s00289-022-04560-0

[9] Umamaheswara, R., Venkatanarayana, B. and Suman, K. N. S., 2019. Enhancement of Mechanical Properties of PLA/PCL (80/20) Blend by Reinforcing with MMT Nanoclay. *Materials Today, 18*, pp. 85-97. Doi:10.1016/j.matpr.2019.06.280

[10] Lyu, J. S., Lee, J. and Han, J., 2019. Development of a biodegradable polycaprolactone film incorporated with an antimicrobial agent via an extrusion process. *Scientific Reports, 9*(1), p. 20236. Doi:10.1038/s41598-019-56757-5

[11] Singsang, W., Rumjuan, P., Ausungnoen, Y., Charentanom, W., Srakaew, N. and Prasoetsopha, N., 2020. Mechanical Properties and Melt Flow Index of Poly (butylene succinate) Blended with a Small Amount of Natural Rubber Compound. *IOP Conferences Series: Materials Science and Engineering, 965*(1), p. 012026. Doi:10.1088/1757-899X/965/1/012026

[12] Faibunchan, P., Nakaramontri, Y., Chueangchayaphan, W., Pichaiyut, S., KummerlÖwe, C., Vennemann, N. and Nakason, C., 2018. Novel Biodegradable Thermoplastic Elastomer Based on Poly(butylene succinate) and Epoxidized Natural Rubber Simple Blends. *Journal of Polymers and the Environment, 26*, pp. 2867-2880. Doi:10.1007/s10924-017-1173-4

[13] Faibunchan, P., Pichaiyut, S., Chueangchayaphan, W., KummerlÖwe, C., Vennemann, N. and Nakason, C., 2019. Influence type of natural rubber on properties of green biodegradable thermoplastic natural rubber based on poly(butylene succinate). *Polymers for Advanced Technologies, 30*(4), pp. 1010-1026. Doi:10.1002/pat.4534

[14] Hemsri, S., Thongpin, C., Moradokpermpoon, N., Niramon, P. and Suppaso, M., 2015. Mechanical Properties and Thermal Stability of Poly(butylene succinate)/ Acrylonitrile Butadiene Rubber Blend. *Macromolecular Symposia, 354*(1), pp. 145-154. Doi:10.1002/masy.20140 0129

[15] Phiri, M. J., Mofokeng, J. P., Phiri, M. M., Mngomezulu, M. and Tywabi-Ngeva, Z., 2023. Chemical, thermal and morphological properties of polybutylene succinate-waste pineapple leaf fibres composites. *Heliyon, 9*(11), p. e21238. Doi:10.1016/j.heliyon.2023.e21238

[16] Calabia, B. P., Ninomiya, F., Yagi, H., Oishi, A., Taguchi, K., Kunioka, M. and Funabashi, M., 2013. Biodegradable Poly(butylene succinate) Composites Reinforced by Cotton Fiber with Silane Coupling Agent. *Polymer, 5*(1), pp. 128-141. Doi:10.3390/polym 5010128

[17] Prasoetopha, N., Thainoi, P., Jinnavat, R., Charerntanom, W., Hasook, A. and Singsang, W., 2020. Morphological and Mechanical Properties of Natural Rubber Compound/ Poly(butylene succinate) Blend. *IOP Conferences Series: Materials Science and Engineering, 840*(1), P. 012013. Doi: 10.1088/1757-899X/840/1/012013

[18] Lotfy, H. R. and Roubik, H., 2023, Water purification using activated carbon prepared from agriculture waste - overview of a recent development. *Biomass Conversion and Biorefinery*, *13*(17), pp. 15577-15590. Doi:10.1007/s13399-021-01618-3

[19] Sujiono, E. H., Zabrian, D., Zurnansyah, Mulyati, Zharvan, V., Samnur, and Humairah, N. A., 2022. Fabrication and characterization of coconut shell activated carbon using variation chemical activation for wastewater treatment application. *Results in Chemistry*, *4*, p. 100291. Doi:10.1016/ j.rechem.2022.100291

[20] Vasilyeva, G. K., Strijakova, E. R. and Shea, P. J., 2006. Use of activated carbon for soil bioremediation. *Soil and Water Pollution Monitoring, Protection and Remediation, 69*, pp. 309–322. Doi:10.1007/978-1-4020-4728-2_20

[21] Gao, J., Liu, D., Xu, Y., Chen, J., Yang, Y., Xia, D., Ding, Y. and Xu, W., 2020. Effects of two types of activated carbon on the properties of vegetation concrete and Cynodon dactylon growth. *Scientific Reports*, *10*(1), p. 14483. Doi:10.1038/s41598-020-71440-w

[22] Omokafe, S.M., Adeniyi, A. A., Igbafen, E. O., Oke, S. R. and Olubambi, P. A., 2020. Fabrication of Activated Carbon from Coconut Shells and its Electrochemical Properties for Supercapacitors. *International Journal of Electrochemical Science, 15*(11), pp 10854-10865. Doi:10.20964/2020.11.10

[23] Nandi, R., Jha, M. K., Guchhait, S. K., Sutradhar, D. and Yadav, S., 2023. Impact of KOH Activation on Rice Husk Derived Porous Activated Carbon for Carbon Capture at Flue Gas alike Temperatures with High CO_2/N_2 Selectivity. *ACS Omega*, *8*(5), pp. 4802-4812. Doi:10.1021/acsomega. 2c06955

[24] Singsang, W., Suetrong, J., Choedsanthia, T., Srakaew, N., Jantrasee, S. and Prasoetsopha, N., 2021. Properties of Biodegradable Poly(butylene succinate) Filled with Activated Carbon Synthesized from Waste Coffee Grounds. *Journal of Materials Science and Applied Energy, 10*(3), pp. 87-95.

[25] Boonpoke, A., Chiarakorn, S., Laosiripojana, N., Towprayoon, S. and Chidthaisong, A., 2011. Synthesis of Activated Carbon and MCM-41 from Bagasse and Rice Husk and their Carbon Dioxide Adsorption Capacity. *Journal of Sustainable Energy and Environment, 2*, pp. 77-81.

[26] Feng, P., Li, J., Wang, H. and Xu, Z., 2020. Biomass-Based Activated Carbon and Activators: Preparation of Activated Carbon from Corncob by Chemical Activation with Biomass Pyrolysis Liquids. *ACS Omega*, *5*(37), pp. 24064-24072. Doi:10.1021/acsomega.0c03494

[27] Molina-Sabio, M. and Rodríguez-Reinoso, F., 2004. Role of chemical activation in the development of carbon porosity. *Colloids and Surfaces A: Physicochemical and Engineering Aspects, 241(1),* pp. 15-25. Doi:10.1016/j.colsurfa.2004.04.007

[28] Shen, Y. and Fu, Y., 2018. KOH-activated rice husk char via CO_2 pyrolysis for phenol adsorption. *Materials Today Energy, 9*, pp. 397-405. Doi:10.1016/j.mtener.2018.07.005

[29] Deng, H., Li, G., Yang, H., Tang, J. and Tang, J., 2010. Preparation of activated carbons from cotton stalk by microwave assisted KOH and K_2CO_3 activation. *Chemical Engineering Journal*, *163(3),* pp. 373-381. Doi:10.1016/j.cej.2010.08.019

[30] Foo, K.Y. and Hameed B.H., 2012. Preparation, characterization and evaluation of adsorptive properties of orange peel based activated carbon via microwave induced K_2CO_3 activation. *Bioresource Technology, 104*, p. 679-686. Doi:10.1016/j.biortech.2011.10.005

[31] Shifa, S. S., Hasan Kanok, M. M., Haque, M. S., Sultan, T., Pritha, K. F., Mubasshira, Al Yeamin, M. and Dipta, S. D., 2024. Influence of heat treatment and water absorption on mechanical properties of cotton-glass fiber reinforced epoxy hybrid composites: An eco-friendly approach for industrial materials. Hybrid Advances, 5, p. 100181. Doi:10.1016/j.hybadv.2024.100181

[32] Somdee, P., Prasoetsopha, N., Detsunhnoen, S., Matnok, S. and Ansari, M. A., 2024. Enhancing Natural Rubber Composites with Spent Coffee Ground: Physical Properties, Odor Absorption, and Processing. Starch – Stärke, p. 2300300. Doi: 10.1002/star.202300300

[33] Khoshraftar, Z. and Ghaemi, A., 2022. Presence of activated carbon particles from waste walnut shell as a biosorbent in monoethanolamine (MEA) solution to enhance carbon dioxide absorption. *Heliyon, 8*(1), p. e08689. Doi:10.1016/j.heliyon.2021.e08689

[34] Siakeng, R., Jawaid, M., Asim, M. and Siengchin, S., 2020. Accelerated Weathering and Soil Burial Effect on Biodegradability, Colour and Textureof Coir/Pineapple Leaf Fibres/PLA Biocomposites. *Polymers (Basel), 12(2),* p. 458. Doi:10.3390/polym12020458

[35] Peñas, M. M., Criado-Gonzalez, M., Martínez de Ilarduya, A., Flores, A., Raquez, J.-M., Mincheva, R., Müller, A. J. and Hernández, R., 2023. Tunable enzymatic biodegradation of poly(butylene succinate): biobased coatings and self-degradable films. Polymer Degradation and Stability, 211, p. 110341. Doi:10.1016/j.polymdegradstab.2023.110341

[36] Zhang, L., Tu, L., Liang, Y., Chen, Q., Li, Z., Li, C., Wang, Z. and Li, W., 2018. Coconut-based activated carbon fibers for efficient adsorption of various organic dyes. *RSC Advances*, *8*(74), pp. 42280-47291. Doi: 10.1039/c8ra08990f

[37] Zhang, Y., Zhao, Y.-P., Qiu, L.-L., Xiao, J., Wu, F.-P., Bai, Y.-H. and Liu, F.-J., 2022. Insights into the KOH activation parameters in the preparation of corncob-based microporous carbon for high-performance supercapacitors. *Diamond and Related Materials, 129,* p. 109331. Doi: 10.1016/j.diamond.2022.109331

[38] Ismail, S.N.S., Ibrahim, N.N.I.N., Rasli, S.N., Majid, N.A., Wahab, N.M.A., Jamal, S.N., Zakaria, S. and Nazir, K., 2022. Reinforcement of Charcoal Activated Carbon (CAC) in Natural Rubber (NR) Compound: in Comparison with Carbon Black. *ASEAN Engineering Journal, 12(2),* pp. 161-167. Doi:10.11113/aej.v12.17224

[39] Nasri, K., Toubal, L., Loranger, É. And Koffi, D., 2022. Influence of UV irradiation on mechanical properties and drop-weight impact performance of polypropylene biocomposites reinforced with short flax and pine fibers. *Composites Part C: Open Access, 9*, p. 100296. Doi: 10.1016/j.jcomc.2022.100296

[40] Veranitisagul, C., Wattanathana, W., Wannapaiboon, S., Hanlumyuang, Y., Sukthavorn, K., Nootsuwan, N., Chotiwan, S., Phuthong, W., Jongrungruangchok, S. and Laobuthee, A., 2019. Antimicrobial, Conductive, and Mechanical Properties of AgCB/PBS Composite System. *Journal of Chemistry, 2019(1),* p. 3487529. Doi: 10.1155/2019/3487529

[41] Luo, X., Li, J., Feng, J., Yang, T. and Lin, X., 2014. Mechanical and thermal performance of distillers grains filled poly(butylene succinate) composites. *Materials and*

Design, 57, pp. 195-200. Doi:10.1016/j.matdes.2013.12.056

[42] Li, J., Luo, X. and Lin, X., 2013. Preparation and characterization of hollow glass microsphere reinforced poly(butylene succinate) composites. *Materials & Design (1980-2015), 46*, pp. 902–909. Doi:10.1016/j.matdes.2012.11.054

[43] Noh, S., Kim, D., Jeong, G., Koo, J.M. and Koo, J., 2024. Highly dispersed biochar as a sustainable filler for enhancing mechanical performance and biodegradation of polybutylene succinate. *Journal of Applied Polymer Science, 141(25),* p. e55539. Doi:10.1002/app.55539

[44] Cappello, M., Rossi, D., Filippi, S., Cinelli, P. and Seggiani, M., 2023. Wood Residue-Derived Biochar as a Low-Cost, Lubricating Filler in Poly(butylene succinate-co-adipate) Biocomposites. *Materials, 16(2),* p. 570. Doi:10.3390/ma16020570

[45] Várdai, R., Lummerstorfer, T., Pretschuh, C., Jerabek, M., Gahleitner, M., Faludi, G., Móczó, J. and Pukánszky, B., 2021. Impact modification of fiber reinforced polypropylene composites with flexible poly(ethylene terephthalate) fibers. *Polymer International, 70*(9), pp. 1367-1375. Doi:10.1002/pi.6210

[46] Ge, F., Wang, X. and Ran, X., 2017. Properties of biodegradable poly(butylene succinate) (PBS)composites with carbon black. *Polymer Science, Series A, 59*(3), pp. 416 – 424. Doi:10.1134/S0965545X17030051

[47] Zulkifli, Z., Daud, Y. M., Zainal, F. F. Abu Hashim, M. F. and Aygörmez, Y., 2023. Effect of Composition on Melt Flow and Density of Polypropylene Copolymer/Kaolin Geo-Filler Composites. Archives of Metallurgy and Materials, 68(1), pp. 369-373. Doi:10.24425/amm.2023.141513

[48] Papadopoulou, K., Klonos, P., Kyritsis, A., Masek, O., Wurzer, C., Tsachouridis, K., Anastasiou, A. and Bikiaris, D., 2023. Synthesis and Study of Fully Biodegradable Composites Based on Poly(butylene succinate) and Biochar. *Polymers, 15,* p. 1049. Doi:10.3390/polym15041049

[49] Zare, Y., 2016. Study of nanoparticles aggregation/agglomeration in polymer particulate nanocomposites by mechanical properties. *Composites Part A: Applied Science and Manufacturing, 84*, pp. 158-164. Doi:10.1016/j.compositesa.2016.01.020

[50] Mohammed Ali, A.S., Hegab, H.M., Almarzooqi, F., Jaoude, M.A., Hasan, S.W. and Banat, F., 2024. Carbon composites for efficient solar-driven atmospheric water harvesting. *Journal of Environmental Chemical Engineering, 12(5),* p. 113319. Doi.10.1016/j.jece.2024.113319

[51] Mrad, H., Alix, S., Migneault, S., Koubaa, A. and Perré, P., 2018. Numerical and experimental assessment of water absorption of wood-polymer composites. *Measurement, 115*, pp. 197-203. Doi:10.1016/j.measurement.2017.10.011

[52] Islam, M. S., Nassar, M., Elsayed, M. A., Jameel, D. B., Ahmad, T. T. and Rahman, M. M., 2023. In Vitro Optical and Physical Stability of Resin Composite Materials with Different Filler Characteristics. *Polymers, 15*(9), p. 2121.

[53] Okolie, O., Kumar, A., Edwards, C., Lawton, L. A., Oke, A., McDonald, S., Thakur, V. K. and Njuguna, J., 2023. Bio-Based Sustainable Polymers and Materials: From Processing to Biodegradation. *Journal of Composites Science, 7(*6), p. 213.

[54] Meereboer, K. W., Misra, M. and Mohanty, A. K., 2020. Review of recent advances in the biodegradability of polyhydroxyalkanoate (PHA) bioplastics and their composites. Green Chemistry, 22(17), pp. 5519-5558. Doi:10.1039/D0GC01647K